

Synthesis of highly luminescent CdTe/ZnO core/shell quantum dots in aqueous solution

Zhimin Yuan · Qian Ma · Aiyu Zhang ·
Yongqiang Cao · Jie Yang · Ping Yang

Received: 28 September 2011 / Accepted: 22 December 2011 / Published online: 10 January 2012
© Springer Science+Business Media, LLC 2012

Abstract The synthesis and photoluminescence (PL) properties of aqueous CdTe/ZnO core/shell quantum dots (QDs) have been investigated by using thioglycolic acid as a capping reagent. The highlighted contribution of the present study was CdTe QDs coated with a ZnO shell by controlling the hydrolysis process of Zn(OAc)₂. The QDs benefitted from overcoming the high lattice mismatch between CdTe and ZnO. The PL peak wavelength of the CdTe/ZnO QDs with high PL quantum yields up to 88% was located in a range between 547 and 596 nm by adjusting the size of CdTe cores and the thickness of ZnO shells. The results of X-ray diffraction analysis and transmission electron microscopy observation indicate that the dot-shaped CdTe/ZnO QDs (566 nm) with an average size of 2.2 nm in diameter belong to the cubic CdTe crystal structure. Due to the passivation of surface defects, it is found that the luminescence decay curves accord with a biexponential decay model of exciton and trap radiation behavior. The average PL lifetimes of CdTe (571 nm) and CdTe/ZnO (596 nm) QDs at room temperature are 27.3 and 35.1 ns, respectively.

Introduction

Semiconductor quantum dots (QDs) have been widely used in the field of optoelectronic and biological applications due to their unique optical properties, such as size-tunable photoluminescence (PL), high PL quantum yield (PLQY), narrow emission line width, superior photostability, and

flexible solution processing [1–3]. During the past decades, there have been many investigations of QD applications for biological imaging, ranging from single-molecule tracking to in vivo imaging and immunological labeling [4, 5]. The QDs with high quality (narrow size distribution, high stability, and high luminescent efficiency) have currently attracted a favorable alternative to organic dyes for light-emitting devices, lasers, and biomedical fluorescent labels [6–8].

As one of the important colloidal II–VI semiconductor nanomaterials, CdTe (bulk one: $E_g = 1.44$ eV at 300 K) QDs are of great interest for both fundamental studies and various promising applications. Although a trioctylphosphine/trioctylphosphine oxide synthetic approach has been regarded as the most successful and well-developed method to prepare highly luminescent II–VI QDs [9, 10], high reaction temperature and the insolubility of obtained QDs extremely restrict their applications. A number of surface functionalization strategies have been developed to make QDs water-soluble and biologically compatible [2, 3, 8, 11], generally resulting in a large decrease of PLQY when the QDs are transferred to water. An ideal approach for producing water-soluble QDs is to directly synthesize QDs in an aqueous medium, in which the products often show relatively low PLQY (3–10%). It is well-known that Murase's [12] and Eychmueller's groups [13] have achieved as-prepared CdTe QDs with an enhanced PLQY of 65% by optimizing the ratio of capping ligand to cadmium. In addition, the size-selective precipitation and selective photochemical etching, and post-preparative methods have been also applied to improve the final PLQY of QDs up to 40% [14].

Surface chemical decoration plays a great role on the PLQY and stability of QDs. For example, the PLQY of CdTe QDs can reach to 70% in the case of dodecylamine/

Z. Yuan · Q. Ma · A. Zhang · Y. Cao · J. Yang · P. Yang (✉)
School of Material Science and Engineering, University of Jinan,
250022 Jinan, People's Republic of China
e-mail: mse_yangp@ujn.edu.cn

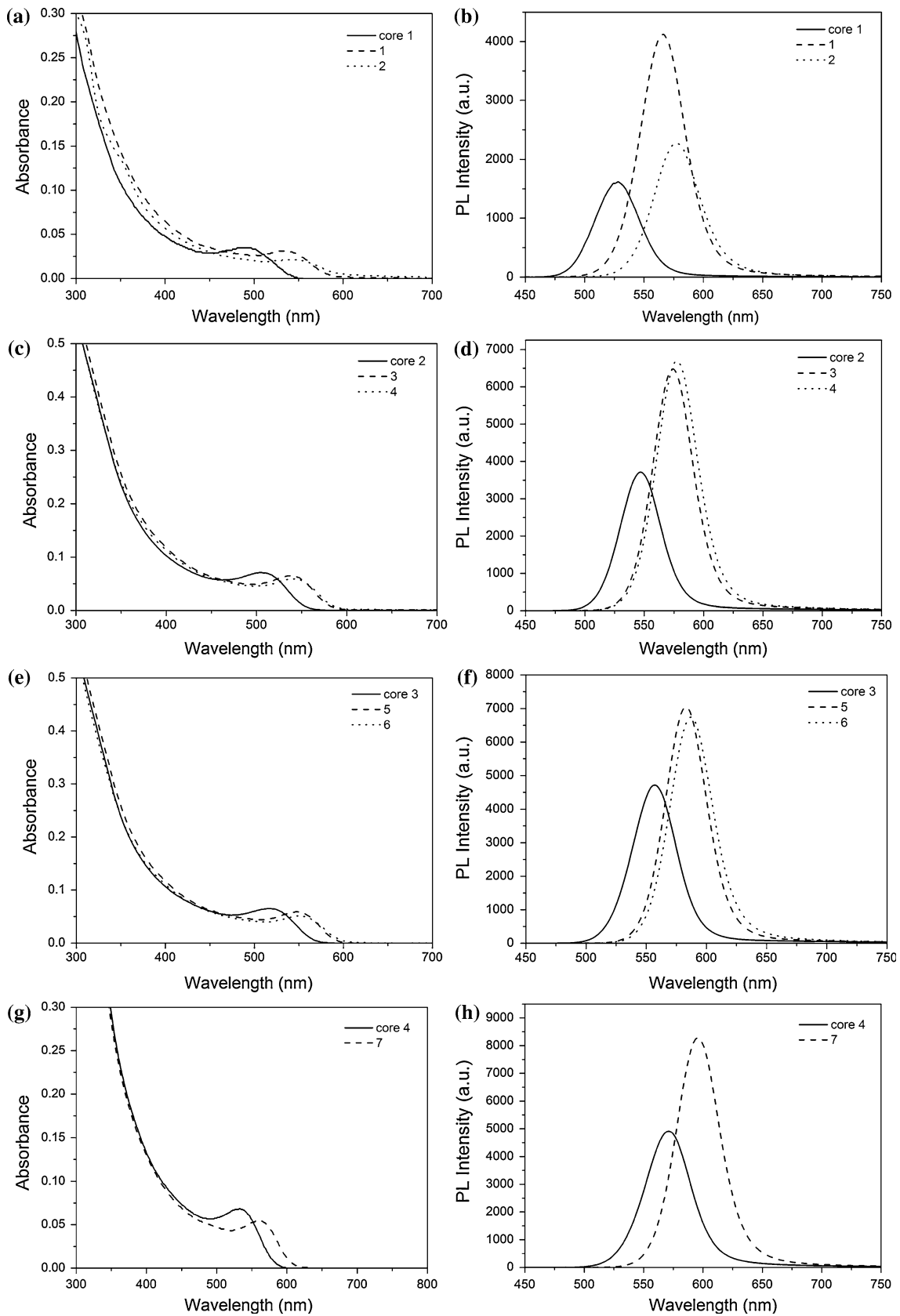


Fig. 1 PL and absorption spectra of TGA-capped CdTe and CdTe/ZnO QDs. **a** Absorption spectra of Core 1 and Samples 1 and 2; **b** PL spectra of Core 1 and Samples 1 and 2; **c** Absorption spectra of Core 2 and Samples 3 and 4; **d** PL spectra of Core 2 and Samples 3 and 4; **e** Absorption spectra of Core 3 and Samples 5 and 6; **f** PL spectra of Core 3 and Samples 5 and 6; **g** Absorption spectra of Core 4 and Sample 7; **h** PL spectra of Core 4 and Sample 7. The preparation conditions and PL properties of TGA-capped CdTe and CdTe/ZnO QDs list in Table 1

trioctylphosphine reactants as a capping ligand [15]. However, their luminescence is unstable under an ambient air atmosphere and the surface properties change by photo-oxidation, as recently investigated by means of synchrotron radiation-excited core-level photoelectron spectroscopy [16]. The epitaxial growth of an inorganic shell with a higher band gap on the surface of QDs is an effective way to improve the spectral characteristics by eliminating both the anionic and cationic dangling bonds on the surface of QDs, normally leading to an enhancement of PLQY. Furthermore, the newly generated nanocrystal systems show novel properties including fine photostability and electronic accessibility [17, 18].

Recently, a series of semiconductor QDs related to CdSe/ZnSe [19], CdSe/CdS [17, 20], and CdSe/ZnS [20, 21] core/shell QDs have been prepared by different organometallic routes. But there are fewer studies on the successful growth of a shell in an aqueous phase [22–24]. In the case of CdTe QDs, Gao's group [22] reported the synthesis of thioglycolic acid (TGA)-capped CdTe/CdS core/shell QDs with the PLQY of 85% by illuminating nitrogen (N₂) saturated QD solutions with low-pressure mercury-rare-gas discharge lamps, in which the CdS shell was achieved by the photodegradation of the TGA stabilizer within a long time (20 days to obtain TGA stabilized CdTe/CdS nanocrystals with the highest PLQY).

ZnO is a significant wide band gap semiconductor (3.37 eV at room temperature) possessing the exciton binding energy of 60 meV, applied in many electronic and optical devices [25, 26]. Nontoxic ZnO exhibits a higher stability against harmful chemical environment compared with ZnS. However, it is difficult to gain the growth of a ZnO shell on CdTe to get a high PLQY because of a large lattice mismatch. The controlling of shell growth kinetics is still expected. In this study, we report on the aqueous synthesis of highly luminescent CdTe/ZnO core/shell QDs with the highest PLQY of 88% without any post-preparative treatment. ZnO shell was successfully grown on the surface of TGA-capped CdTe QDs by the hydrolysis of Zn(OAc)₂. Because of the passivation of surface defects, the average PL lifetimes increase from 27.3 ns for CdTe (571 nm) to 35.1 ns for CdTe/ZnO (596 nm). The epitaxial growth of the ZnO shell was confirmed by X-ray diffraction (XRD) analysis and PL spectrum measurement.

Experimental procedures

Chemicals

All chemicals used in the current experiments were used as received without further purification. TGA (C₂H₄O₂S, 99%), Tellurium powder (Te, 99%), CdCl₂·2.5H₂O (98%), zinc acetate (99%), and sodium borohydride (NaBH₄, 96%) were purchased from Shanghai Chemical Reagents Company. Rhodamine 6G was supplied by Aldrich. The pure water was obtained from a Milli-Q synthesis system.

Synthesis of water-soluble TGA-capped CdTe QDs

Water-soluble TGA-capped CdTe QDs were prepared by a soft procedure according to the report in literature [27]. The solution of sodium hydrogen telluride (NaHTe) was first prepared by the reaction of NaBH₄ and Te powder (the molar ratio of NaBH₄:Te = 5:1). In brief, 37.8 mg (1 mmol) of NaBH₄ and 25.5 mg (0.2 mmol) of Te powder were added into a small two-neck flask, pumping off the air in the system for 30 min and flowing with N₂. 91.3 mg (0.4 mmol) of CdCl₂·2.5H₂O and 41.56 μL (0.6 mmol) of TGA was mixed in 25 mL of water with stirring. The pH of Cd²⁺ and TGA solution was adjusted into 11 by using 1 M NaOH solution under vigorous stirring. After the solution was degassed by high-purity N₂ bubbling for 30 min, an oxygen-free NaHTe solution was injected. Finally, the mixture with a faint yellow color was refluxed at 100 °C for various times to create CdTe QDs with different sizes.

Synthesis of TGA-capped CdTe/ZnO core/shell QDs

The synthesis of CdTe/ZnO core/shell QDs was described as follows:

0.0175 g (0.08 mmol) of zinc acetate was dissolved in 8 mL of pure water to get solution A (0.01 M of Zn²⁺). 10 mL of crude CdTe QDs were added into a three-necked flask and heated up to 100 °C to get solution B. Then, 2 or 4 mL of solution A was injected into solution B using a speed of 0.2 mL/min. The mixture was refluxed for 1 h to create CdTe/ZnO QDs. The obtained CdTe/ZnO QDs were filtered by using a 0.2 μm filter. To get tunable PL peak wavelength from green to red region, CdTe/ZnO QDs with various core sizes and shell thicknesses were prepared by adjusting preparation parameters.

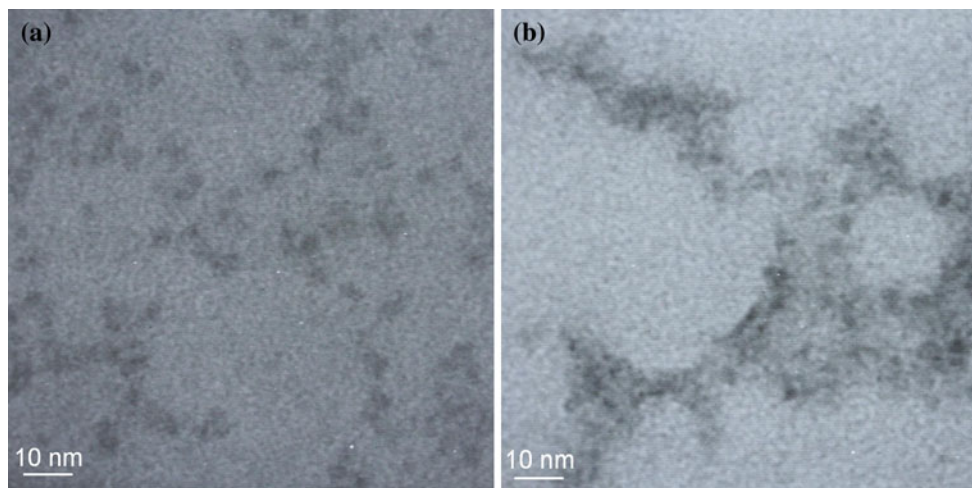
Characterization

All spectral measurements were performed at room temperature under ambient conditions. The absorption spectra were recorded on a HITACHI U-4100 UV–VIS–NIR Spectrophotometer. PL spectra were recorded by using a HITACHI

Table 1 Preparation conditions and properties of TGA-capped CdTe and CdTe/ZnO QDs

Sample	QD kind	Reflux time (h)	Amount of Zn(OAc) ₂ added (mL) ^a	PL peak wavelength (nm)	First excitonic absorption peak(nm)	FWHM (nm)	PLQY (%)
<i>Core 1</i>	CdTe	N/A	N/A	527	490	45.1	43.5
1	CdTe/ZnO	1	2	566	534	44.9	67.4
2	CdTe/ZnO	2	4	577	543	45.0	56.7
<i>Core 2</i>	CdTe	N/A	N/A	547	506	39.4	57.1
3	CdTe/ZnO	1	2	574	539	38.4	84.6
4	CdTe/ZnO	2	4	578	542	39.5	73.2
<i>Core 3</i>	CdTe	N/A	N/A	557	518	41.8	63.1
5	CdTe/ZnO	1	2	583	550	39.7	86.4
6	CdTe/ZnO	2	4	587	553	42.1	78.6
<i>Core 4</i>	CdTe	N/A	N/A	571	532	45.6	62.4
7	CdTe/ZnO	1	2	596	560	43.2	88.2

^a The concentration of Zn(OAc)₂ in solutions is 0.01 M

**Fig. 2** TEM images of CdTe core QDs (2.0 nm) and the resulting CdTe/ZnO core/shell QDs (2.2 nm): **a** Core 1; **b** Sample 1

F-4600 Fluorescence Spectrophotometer. The PLQY of QDs was estimated in comparison with Rhodamine 6G (assuming the PLQY of 95%) in ethanol solution. The sizes of QDs were both determined by transmission electron microscopy (TEM, Hitachi H9000NA) observation and the calculation according to the first excitonic peak [28]. Samples were precipitated by 2-propanol and dried in a vacuum oven for XRD analysis (Bruker D8 diffractometer). PL lifetime measurements were carried out by using a time-correlated single-photon-counting spectrofluorometer system (Fluorocube-01, JY-IBH, Horiba).

Results and discussion

PL properties of CdTe and CdTe/ZnO QDs

The PLQY of QDs can be estimated by using Rhodamin 6G as a reference [29] by the equation $\Phi = \Phi_{\text{ref}} (S/S_{\text{ref}})$

$(A/A_{\text{ref}}) (n^2/n_{\text{ref}}^2)$, where Φ is the PLQY of sample, Φ_{ref} is the PLQY of the standard Rhodamin 6G, S is the integration of the fluorescence emission, A is the absorbance at the excitation wavelength, all the absorbance values of the samples at excitation wavelength were less than 0.15 for our samples, n is the refractive index of the solution [30].

Figure 1 shows typical absorption and PL spectra of TGA-capped CdTe and CdTe/ZnO QDs prepared in an aqueous solution. Table 1 summarizes preparation conditions and properties of TGA-capped CdTe and CdTe/ZnO QDs in detailed. In the current experiments, CdTe QDs with various sizes were successfully fabricated. Four kinds of the CdTe QDs with PL peak wavelength of 527 (Core 1 shown in Table 1), 547 (Core 2 shown in Table 1), 557 (Core 3 shown in Table 1), and 571 nm (Core 4 shown in Table 1) were used to fabricate CdTe/ZnO QDs for the purpose of investigating the effect of ZnO shell thickness on the optical and

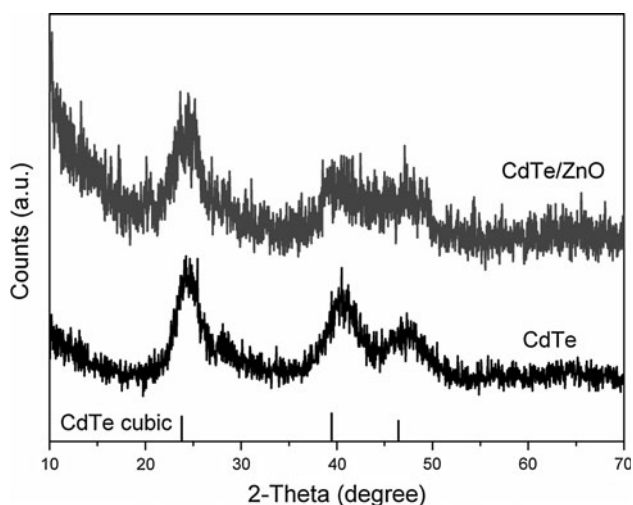


Fig. 3 XRD patterns of TGA-capped CdTe (Core 1) and CdTe/ZnO QDs (Sample 1). The lines on the *bottom* show the standard diffractions of cubic CdTe

structural properties. The size and concentration of the CdTe cores are 2 nm and 7.6×10^{-7} mol L⁻¹ for Core 1, 2.5 nm, and 1.7×10^{-6} mol L⁻¹ for Core 2, 2.8 nm, and 1.0×10^{-6} mol L⁻¹ for Core 3, and 3.0 nm and 7.9×10^{-7} mol L⁻¹ for Core 4. The size of CdTe QDs was estimated by the following equations [28]:

$$D = (9.8127 \times 10^{-7})\lambda^3 - (1.7147 \times 10^{-3})\lambda^2 + (1.0064)\lambda - (194.84) \quad (1)$$

$$\varepsilon = 10043(D)^{2.12} \quad (2)$$

$$A = \varepsilon CL \quad (3)$$

where D (nm) is the diameter of a given QD sample, λ (nm) is the wavelength of the first excitonic absorption peak of the corresponding sample, ε is extinction coefficient per mole of particles, A is the absorbance at the first exciton absorption peak of a given sample, C is the molar concentration (mol/L) of the QD sample, L is the path length (cm) of the irradiation beam used for recording the absorption spectrum.

Being coated with a ZnO shell, red-shift of absorption and PL spectra was observed. For example, Core 1 (CdTe QDs) and Sample 2 (CdTe/ZnO core/shell QDs) revealed PL peak wavelengths of 527 and 577 nm, respectively. The size of CdTe cores drastically affected the PL spectra of CdTe/ZnO core/shell QDs. Furthermore, with increasing the ZnO shell thickness, a red-shift was observed for both the absorption and PL spectra of CdTe/ZnO core/shell QDs as shown in Fig. 1. This is ascribed to the effect of the effect of the thickness on the band gap of the core/shell QDs. Taking account of the single emission peak in PL spectra and no corresponding ZnO absorption peaks in

absorption ones, no separate nucleation process of ZnO QDs occurs. This result was supported by the results from XRD analysis as we discussed later.

In addition, the PLQY of CdTe QDs was greatly enhanced with the overcoating of the ZnO shell. For example, the PLQY of Core 4 (CdTe cores) was 62.4% while that of Sample 7 was 88% (CdTe/ZnO core/shell QDs). The increased PLQY is mainly attributed to the passivation surface defects on the cores. Namely, the decrease of PL quenching centers resulted in the improvement of PLQY. The high PLQY is associated with relatively slow nonradiative recombination rates, implying low defect concentration staying on the high quality CdTe/ZnO core/shell QDs.

As illustrated in Table 1, compared with Core 1 with a PLQY of 43.5%, the PLQY of CdTe/ZnO core/shell QDs was first increased into 67.4% (Sample 1), and then decreases to 56.7% (Sample 2). This phenomenon was also observed for Cores 2 and 3 coated with a ZnO shell. The decreased PLQY of the thicker-shelled CdTe/ZnO QDs may be originated from several mechanisms: (i) a weaker quantum confinement effect due to their larger particle sizes [31, 32] and (ii) the strain released through the formation of dislocation in the shell with increasing shell thickness, as observed in the well-developed CdSe/ZnS core/shell system [20, 33]. With the overcoating of ZnO shells on the CdTe cores, the full width at half-maximum (FWHM) of PL spectra of CdTe/ZnO core/shell QDs decreased as listed in Table 1, which demonstrates the narrow size distribution of the core/shell particles.

Figure 2a shows the TEM image of CdTe QDs (Core 1) with an average size of 2 nm in diameter which is similar to that estimated by using Eqs. 1–3. Figure 2b shows the TEM image of Sample 1 (CdTe/ZnO core/shell QDs) with an average diameter of is 2.2 nm. TEM images represent the approximate theoretical thickness calculated from the amount of injected stock solution, which gives strong evidence for the epitaxial growth of ZnO on the surface of CdTe cores without the independent nucleation of ZnO. It is noted that the morphologies of CdTe and CdTe/ZnO QDs are nearly dot-shaped.

The typical XRD patterns of TGA-capped CdTe (Core 1) and CdTe/ZnO (Sample 1) QDs are depicted in Fig. 3. The characteristic zinc blend planes of 111, 220, and 311 locating at 24.40°, 41.60°, and 47.90° for CdTe have been obviously observed. The position of XRD peaks of CdTe QDs matched well with those of bulk CdTe cubic structure. With the further overgrowth of the ZnS shell on the surface of CdTe, the diffraction peak positions have no significant shift. Therefore, CdTe/ZnO QDs have the same crystal structure as CdTe QDs.

Fig. 4 Time-resolved luminescence decay curves (measured at maximum emission peak, $\lambda_{\text{ex}} = 370$ nm) of TGA-capped CdTe and CdTe/ZnO QDs. **a** Core 1 and Samples 1 and 2; **b** Core 2 and Samples 3 and 4; **c** Core 3 and Samples 5 and 6; **d** Core 4 and Sample 7. Reproduced curves for data shown in Table 2 are plotted as thin gray lines

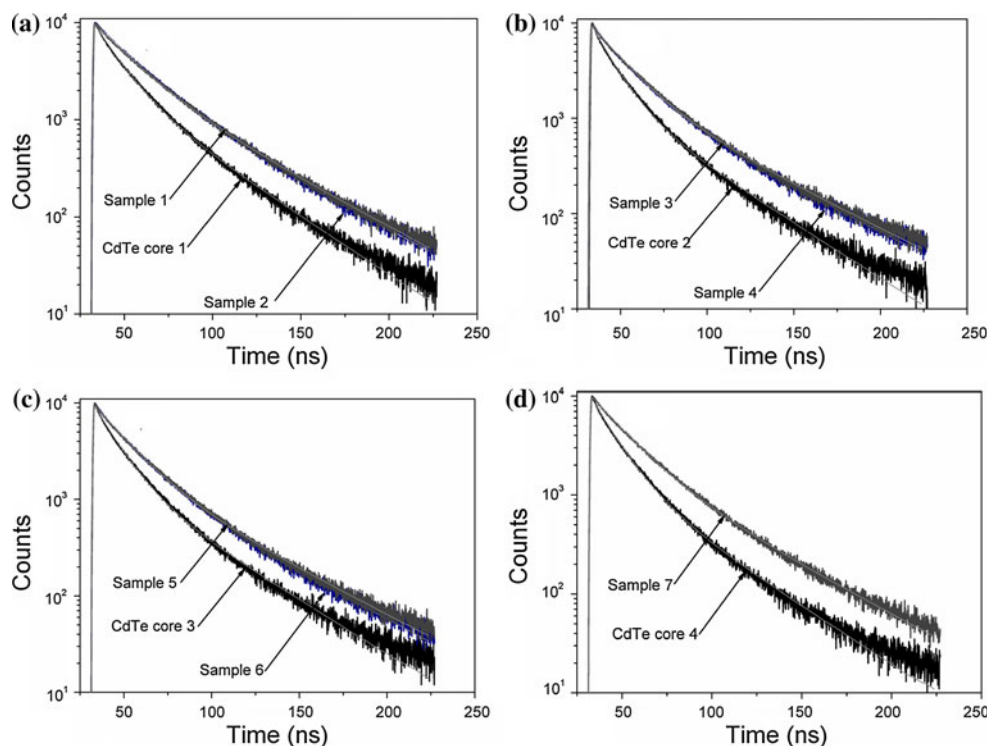


Table 2 Time constants τ_1 and τ_2 , components B_1 and B_2 , average lifetime τ of CdTe and CdTe/ZnO QDs

Sample	τ_1 (ns)	τ_2 (ns)	B_1	B_2	τ (ns)
Core 1	12.79	34.63	49.2	50.8	28.9
1	20.05	43.81	51.84	48.16	36.0
2	19.62	44.52	49.63	50.37	37.0
Core 2	11.26	35.25	55.83	44.17	28.4
3	16.82	45.54	54.91	45.09	36.6
4	17.29	46.87	55.28	44.72	37.6
Core 3	12.16	36.66	55.91	44.09	29.4
5	17.46	44.01	56.94	43.06	34.9
6	17.65	45.46	56.21	43.79	36.2
Core 4	12.09	34.58	57.67	42.33	27.3
7	18.48	44.29	56.93	43.07	35.1

PL lifetime of CdTe and CdTe/ZnO QDs

Luminescence decay kinetics provides additional important information on the recombination of photoinduced carriers in the QDs. The PL decay time is monitored under the excitation wavelength at 370 nm. Figure 4 shows the PL decay curves of CdTe QDs and CdTe/ZnO core/shell QDs: (a) Core 1 and Samples 1 and 2, (b) Core 2 and Samples 3 and 4, (c) Core 3 and Samples 5 and 6, and (d) Core 4 and Sample 7. Reproduced curves for data shown in Table 2 are plotted as thin gray lines. The recorded decay curves were fitted with a multiexponential function by least squares fitting. If the PL intensity decreased to 1/e times of its initial value, these PL decay times (i.e., the exciton

decay times, $\tau_{1/e}$) can be used as a standard parameter to estimate the lifetimes. The decay curves can be well-fitted to a biexponential model described by the equation as follows:

$$F(t) = A + B_1 \exp(-t/\tau_1) + B_2 \exp(-t/\tau_2) \tag{4}$$

where τ_1 and τ_2 ($\tau_1 < \tau_2$) represent the time constants, and B_1 and B_2 represent the amplitudes of the fast and slow components, respectively. The average decay time τ was calculated by using the equation below [34]:

$$\tau = (B_1\tau_1^2 + B_2\tau_2^2)/(B_1\tau_1 + B_2\tau_2) \tag{5}$$

the values of the parameters B_1 , B_2 , τ_1 , τ_2 , and τ are summarized in Table 2.

The shorter lifetime can be attributed to the exciton recombination, while the longer ones can be associated with the involvement of surface states in the carrier recombination process [35, 36]. It is found that the exciton decay time increased remarkably with the deposition of a ZnO shell on CdTe cores. For example, the average decay time of Core 1 (CdTe QDs) is 28.9 ns, while those of Samples 1 and 2 (CdTe/ZnO QDs) are 36.0 and 37.0 ns, respectively. The result indicates that the intrinsic recombination of QDs changes obviously because of the deposition of a ZnO shell. The longer decay time is assigned to the thermal detrapping of the electrons from the surface states to the conduction band since such thermal activation could enhance the decay time of the band-edge emission. The formation ZnO shells resulted in a high PLQY due to the removal of surface defects or the quenching non-radiative exciton recombination routes that is related to the thermal activation of the electrons.

Conclusion

A facile and cheap method has been developed to synthesize aqueous TGA-capped CdTe/ZnO core/shell QDs with a high PLQY under the moderate temperature around 100 °C. The emission wavelength of CdTe/ZnO QDs was adjusted from 547 to 596 nm by changing the size of CdTe cores and the thickness of a ZnO shell. Because of the ZnO shell, the PLQY of the CdTe/ZnO QDs at room temperature reached up to 88%. The average PL lifetime of the CdTe/ZnO QDs were increased gradually. Since the soft processing and excellent PL properties, these aqueous CdTe/ZnO QDs are great potential in the biolabeling and other applications.

Acknowledgements This study was supported in part by the Program for Taishan Scholars, projects from National Natural Science Foundation of China (21071061), and projects from Natural Science Foundation of Shandong Province (ZR2010EZ001), Outstanding Young Scientists Foundation Grant of Shandong Province (BS2010CL004), and Graduate Student Innovation Foundation of University of Jinan (YCX10018).

References

- Colvin VL, Schlamp MC, Alivisatos AP (1994) *Nature* 370:354
- Bruchez MJ, Moronne M, Gin P, Weiss S, Alivisatos AP (1998) *Science* 281:2013
- Chan WCW, Nie SM (1998) *Science* 281:2016
- Dahan M, Levi S, Luccardini C, Rostaing P, Riveau B, Triller A (2003) *Science* 302:442
- Dubertret B, Skourides P, Norris DJ, Noireaux V, Brivanlou AH, Libchaber A (2002) *Science* 298:1759
- Somers RC, Bawendi MG, Nocera DG (2007) *Chem Soc Rev* 36:579
- Burda C, Chen X, Narayanan R, El-Sayed MA (2005) *Chem Rev* 105:1025
- Michalet X, Pinaud FF, Bentolila LA, Tsay JM, Doose S, Li JJ, Sundaresan G, Wu AM (2005) *Science* 307:538
- Murray CB, Norris DJ, Bawendi MG (1993) *J Am Chem Soc* 115:8706
- Qu L, Peng X (2002) *J Am Chem Soc* 124:2049
- Mattoussi H, Mauro JM, Goldman ER, Anderson GP, Sundar VC, Mikulec FV, Bawendi MG (2000) *J Am Chem Soc* 122:12142
- Li C, Murase N (2005) *Chem Lett* 34:92
- Shavel A, Gaponik N, Eychmueller A (2006) *J Phys Chem B* 110:19280
- Gaponik N, Talapin DV, Rogach AL, Hoppe K, Shevchenko EV, Kornowski A, Eychmueller A, Weller H (2002) *J Phys Chem B* 106:7177
- Talapin DV, Haubold S, Rogach AL, Kornowski A, Haase M, Weller H (2001) *J Phys Chem B* 105:2260
- Lobo A, Borchert H, Talapin DV, Weller H, Moeller T (2006) *Colloid Surf A Physicochem Eng Asp* 286:1
- Peng X, Schlamp MC, Kadavanich AV, Alivisatos AP (1997) *J Am Chem Soc* 119:7019
- Rockenberger J, Troger L, Rogach AL, Tischer M, Grundmann M, Eychmuller A, Weller H (1998) *J Chem Phys* 108:7807
- Danek M, Jensen KF, Murray CB, Bawendi MG (1996) *Chem Mater* 8:173
- Dabbousi BO, Rodriguez-Viejo J, Mikulec FV, Heine JR, Mattoussi H, Ober R, Jensen KF, Bawendi MG (1997) *J Phys Chem B* 101:9463
- Wang H, Nakamura H, Uehara M, Yamaguchi Y, Miyazaki M, Maeda H (2005) *Adv Funct Mater* 15:603
- Bao H, Gong Y, Li Z, Gao M (2004) *Chem Mater* 16:3853
- Lin YW, Hsieh MM, Liu CP, Chang HT (2005) *Langmuir* 21:728
- Wang Y, Tang Z, Correa-Duarte MA, Pastoriza-Santos I, Giersig M, Kotov NA, Liz-Marzan LM (2004) *J Phys Chem B* 108:15461
- Fu YS, Du XW, Kulinich SA, Qiu JS, Qin WJ, Li R, Sun J, Liu J (2007) *J Am Chem Soc* 129:16029
- Houskova V, Stengl V, Bakardjeva S, Murafa N, Kalendova A, Oplustil F (2007) *J Phys Chem A* 111:4215
- Yuan Z, Zhang A, Cao Y, Yang J, Zhu Y, Yang P (2011) *J Fluoresc*. doi:10.1007/s10895-011-0937-9
- Yu WW, Qu LH, Guo WZ, Peng XG (2003) *Chem Mater* 15:2854
- Huang ZL, Lei H, Li N, Qiu ZR, Wang HZ, Guo JD, Luo Y, Zhong ZP, Liu XF, Zhou ZH (2003) *J Mater Chem* 13:708
- Peng H, Zhang L, Soeller C, Travas-Sejdic J (2007) *J Lumin* 127:721
- Zhong X, Feng Y, Knoll W, Han M (2003) *J Am Chem Soc* 125:13559
- Norris D, Bawendi M (1996) *Phys Rev B* 53:16338
- Hines MA, Guyot-Sionnest P (1996) *J Phys Chem* 100:468
- Jones M, Nedeljkovic J, Ellingson RJ, Nozik AJ, Rumbles G (2003) *J Phys Chem B* 107:11346
- Zhang JY, Wang XY, Xiao M (2002) *Opt Lett* 27:1253
- Wang XY, Qu L, Zhang JY, Peng XG, Xiao M (2003) *Nano Lett* 3:1103